Dry reforming of methane at high pressure in a fixed-bed reactor with axial temperature profile determination

Lukas Tillmann,[1] Jonas Schulwitz,[1] André van Veen,[2] and Martin Muhler*[1]

[1] *Prof. M. Muhler, L. Tillmann, J. Schulwitz*
Ruhr-University Bochum, Laboratory of Industrial Chemistry
Universitätsstr. 150, 44801 Bochum (Germany)

[2] *Prof. A. C. van Veen*
University of Warwick, School of Engineering
Library Road, CV4 7AL Coventry (United Kingdom)

[*] E-mail: muhler@techem.rub.de

Keywords

Methane, carbon dioxide, dry reforming, high pressure, axial temperature profile, nickel, spinel

Abstract

A continuously operated flow setup with fixed-bed reactor and online gas analysis enabled kinetic investigations of catalysts for the carbon dioxide reforming of methane under industrially relevant conditions at temperatures up to 1000 °C and at pressures up to 20 bar. A coaxial reactor design consisting of an inner- and an outer highly alloyed steel tube allowed obtaining axial temperature profiles by means of a moveable thermocouple. A $NiAl_2O_4$-based catalyst was tested at 820 °C and pressures of 1, 10 or 20 bar and compared to a conventional Ni catalyst used for steam reforming of methane. A significant cold spot was detected even when using only 10 mg of catalysts diluted in 1 g of silicon carbide. The specifically designed $NiAl_2O_4/Al_2O_3$ dry reforming catalyst with a high dispersion of the active Ni^0 phase was found to be far superior to the conventional steam reforming catalyst.

Graphical abstract

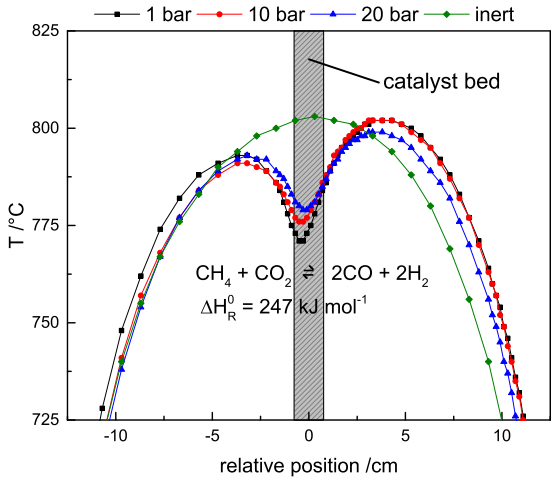

1 Introduction

The dry reforming of methane (DRM) (eq. 1) is discussed as a promising route to generate synthesis gas with high CO content and a H_2/CO ratio close to unity.

$$CH_4 + CO_2 \rightleftharpoons 2CO + 2H_2 \qquad \Delta H_R^0 = 247\ \text{kJ mol}^{-1} \qquad (1)$$

The most obvious applications for syngas produced by DRM are Fischer-Tropsch synthesis (FTS) of long-chain hydrocarbons as synthetic fuel and oxo synthesis of aldehydes [1-5]. Due to a more economically feasible transportation of liquid products over long distances as opposed to gaseous intermediates, a combined facility for DRM and FTS could be utilized to exploit otherwise unattractive stranded natural gas fields in remote locations [3]. A second potential application is the reforming of biogas, which is naturally rich in CH_4 and CO_2 [4,6,7]. Since both reactants are potent greenhouse gases, there is additional motivation to establish the DRM reaction on the industrial scale to mitigate their negative environmental impact [1,5,6]. It is widely accepted that the increased tendency for deposition of solid carbon through the Boudouard equilibrium (eq. 2) and methane pyrolysis (eq. 3) and the associated loss of catalytic activity is one of the strongest drawbacks of DRM in comparison to syngas generation via steam reforming of methane (SRM, eq. 5) [1,2,4-8]. Furthermore, the H_2/CO ratio can be lowered by the reverse water-gas shift reaction (rWGS) (eq. 4) subsequent to DRM.

$$2CO \rightleftharpoons C + CO_2 \qquad \Delta H_R^0 = -172\ \text{kJ mol}^{-1} \qquad (2)$$

$$CH_4 \rightleftharpoons C + 2H_2 \qquad \Delta H_R^0 = 75\ \text{kJ mol}^{-1} \qquad (3)$$

$$H_2 + CO_2 \rightleftharpoons H_2O + CO \qquad \Delta H_R^0 = 41\ \text{kJ mol}^{-1} \qquad (4)$$

$$CH_4 + H_2O \rightleftharpoons CO + 3H_2 \qquad \Delta H_R^0 = 206\ \text{kJ mol}^{-1} \qquad (5)$$

Identification of catalysts for DRM suitable both from a chemical and an economic point of view requires investigating readily available transition metal-based materials with low costs, usually containing Ni as the active species, at industrially relevant conditions. When syngas is to be used for FTS, its production by DRM needs to be conducted at elevated pressure to save the investment and operation costs of downstream compression units [6,8]. In the pool of currently available research articles, this aspect is too frequently not taken into account, since new challenges for the setup applied for catalyst testing are imposed. Thus, academic studies can identify catalysts with outstanding performance at atmospheric pressure but may lack information on their applicability in actual chemical plants operated at high pressure. In addition, there are thermodynamic implications: under pressurized conditions, the equilibrium degree of conversion is limited, while the formation of coke (eq. 2) is favored according to the Le Chatelier principle [4,6,9].

The effect of pressure on the activity of a $NiAl_2O_4/Al_2O_3$ catalyst under dry reforming conditions was studied by applying pressures between 1 and 20 bar. This type of catalyst was selected, because a high dispersion of elemental Ni can be achieved by reducing the spinel precursor as demonstrated by X-ray diffraction (XRD), temperature-programmed reduction (TPR), and hydrogen chemisorption, resulting in a highly active catalyst [10,11].

2 Experimental

2.1 Catalyst preparation

$NiAl_2O_4/Al_2O_3$ was prepared by dissolving 3.68 g $Ni(NO_3)_2{\cdot}6H_2O$ (Alfa Aesar) in 15 mL HPLC-grade water and adding the solution to 4.06 g Al_2O_3 (Aluminiumoxid C, Degussa) in a round-bottom flask. The suspension was stirred for 2 h at 60 °C. Subsequently, water was removed in a rotary evaporator. The impregnated Al_2O_3 support

was dried in an oven at 100 °C, then ground in a mortar dish. In order to remove the nitrate precursor and to induce spinel formation, the sample was finally calcined at 800 °C in synthetic air (20 % O_2 in Ar) for 2 h using a heating rate of 10 K min^{-1}. Complete decomposition of nitrate and removal of water was demonstrated by TG-MS analysis. A conventional Ni-based steam reforming catalyst was used as received. Both samples were pressed, crushed and sieved to yield grain sizes of 250-350 µm.

2.2 Catalyst characterization

A sample of the calcined $NiAl_2O_4/Al_2O_3$ catalyst precursor was ground in a mortar dish to avoid preferred orientations and investigated by powder XRD using Cu K_α radiation in a 2θ range from 5° to 80°. The XRD measurements were also performed with a sample that had been reduced at 850 °C for 30 min using a flow of 10 % H_2 in N_2 and a total flow of 100 mL min^{-1}, as well as with a catalyst after reaction that had been exposed to DRM conditions for 15 h. The Ni content was assessed by ICP-OES. The specific surface area of the calcined catalyst was determined by N_2 physisorption at 77.15 K using a NOVA 2000 setup (Quantachrome Instruments). TPR measurements were conducted in a quartz cell. The sample was heated in 84.1 mL min^{-1} of 4.6 % H_2 in Ar with a constant rate of 6 K min^{-1} up to 850 °C. H_2 consumption was monitored by means of a thermal conductivity detector (TCD, Hydros, Rosemount). The H_2 chemisorption capacity of a reduced $NiAl_2O_4/Al_2O_3$ sample was analyzed in a static volumetric setup (Autosorb, Quantachrome Instruments) to calculate active metal surface area, dispersion and average crystallite size using the bracketing method.

2.3 Catalytic DRM tests

The catalytic DRM activity was assessed in a flow setup equipped with a tubular steel reactor with an inner diameter of 9.4 mm containing a coaxial inner steel tube of 4 mm diameter. The annular gap of 2.7 mm between both tubes was loaded with a fixed bed containing 10 mg catalyst diluted in 1 g of green SiC as inert material which was held in place on both sides by quartz wool plugs. All tubes within the hot zone were made of high temperature-resistant highly alloyed steel (nickel-iron-chromium solid solution alloy 800H) coated with Silcolloy 1000 for passivation. A moveable K-type thermocouple in the inner tube was employed for monitoring the bed temperature and measuring axial temperature profiles at steady state. Each profile was determined by measuring the temperature at up to a total of 102 positions. The product gas composition was analyzed using an Agilent 3000 Micro-GC equipped with PLOT-Q and Molsieve 5A PLOT columns and a TCD. Pressure was regulated using a dome-loaded backpressure regulator (ER 3000, Emerson).

Catalytic activity was determined by first reducing the catalyst in a flow of 10 % H_2 in N_2 (purity 99.999 % each) and a total flow of 100 mL min^{-1} with a heating rate of 10 K min^{-1} up to the final temperature of 850 °C, which was held for 30 min. Then, temperature was lowered to an oven temperature of 820 °C and the reactor was flushed with pure nitrogen. The gas flow was then switched to a mixture of CH_4 (purity 99.995 %), CO_2 (purity 99.995 %) and N_2 in a ratio of 7: 9.5: 83.5 and a total flow of 490 mL min^{-1}. These conditions were held for 5 h at atmospheric pressure, 10 bar and 20 bar.

3 Results

3.1 Characterization

The $NiAl_2O_4/Al_2O_3$ catalyst precursor was characterized by various methods to confirm the initial spinel formation and the subsequent reduction, which gives rise to supported Ni^0 nanoparticles. XRD patterns of the calcined precursor, the reduced sample and a catalyst after reaction are shown in Fig. 1. Three crystalline phases were found in the calcined precursor: NiO (PDF 01-089-7101), $NiAl_2O_4$ (PDF 00-010-0339) and γ-Al_2O_3 (PDF

00-029-0063). NiO exhibits well separated reflections with relatively low intensity, while the reflections of $NiAl_2O_4$ and γ-Al_2O_3 overlap due to the common cubic crystal structure. The reflections of γ-Al_2O_3 should be detected at slightly larger angles, since the cell parameters (a=b=c=7.924 Å) are smaller than those of the $NiAl_2O_4$ spinel (a=b=c=8.048 Å). However, peaks are found to be at positions in between the expected 2θ angles for both phases, indicating strong contributions from both the spinel and the alumina support that lead to fully overlapping peaks. The presence of the $NiAl_2O_4$ phase is further demonstrated by the blue color of the calcined catalyst precursor. Reduction in H_2 removes the NiO phase and shifts the positions of the overlapping peaks towards larger angles, while their intensity is lowered, indicating that the spinel phase has either only small or no contributions at all in case of the reduced sample, which is in good agreement with the observation of an elemental Ni^0 phase (PDF 01-070-1849) originating from the reduction of NiO and of the spinel. Thus, the reduced catalyst consists of Ni^0 nanoparticles embedded in γ-Al_2O_3. The catalyst after 15 h of DRM exhibits the same diffraction pattern with the additional (002) reflection of graphitic carbon at 26.5 ° (PDF 00-056-0159) and some sharp reflections caused by SiC particles that were not fully separated when sieving the catalyst after reaction. Remarkably, both the reduced and the catalyst after retain reduced Ni^0 even when handled in air.

The results of the TPR experiments are shown in Fig. 2. There is a minor reduction peak above 400 °C that reaches a plateau at 544 °C, which can be attributed to the reduction of NiO as observed in the XRD pattern. A second and more intense reduction peak occurs at 799 °C, which indicates the reduction of the $NiAl_2O_4$ spinel phase. Reducing this phase is more demanding, since the spinel matrix stabilizes Ni^{2+} strongly. Upon reaching the highest temperature of 850 °C, H_2 consumption continues to decrease with time. The integration of the H_2 TPR profile indicates that full reduction was achieved. In addition, the absence of other Ni phases apart from Ni^0 in the XRD pattern of the reduced sample confirms that reduction is complete under these conditions.

Further characterization results are summarized in Table 1. The Ni loading is slightly lower than the nominal value of 15% we aimed at for during synthesis, while the specific surface area reaches 126 m^2g^{-1}. H_2 chemisorption experiments yield a Ni surface area of 1.8 m^2g^{-1} and 2.0% dispersion. However, the calculated average crystallite size is rather large amounting to 50.1 nm under assumption of a perfect spherical shape and particles of equal size. In addition, Ni^0 surfaces may be partly covered by the Al_2O_3 matrix and thus offer less sites for adsorption. Indeed, an analysis of the Ni^0 (200) reflection at 51.8 ° in the XRD pattern of the reduced sample by employing the Scherrer equation suggests an average particle diameter of only 14.9 nm.

3.2 Catalytic testing

The achieved degrees of conversion with $NiAl_2O_4/Al_2O_3$ during 5 h on stream under pressures of 1, 10 and 20 bar are shown in Fig. 3 (top) together with the product distribution (bottom). Catalyst charges as low as 10 mg enable an impressive initial 74% conversion of CH_4 at both 1 and 10 bar, while conversion at 20 bar is significantly lowered to 62%. Over the course of 5 h, these values gradually decrease to 72, 69 and 60%, respectively. The loss of activity is accompanied by a significant formation of solid carbon under pressurized conditions that can be monitored by the incomplete carbon balance. In fact, the reason for limiting the reaction time to only 5 h is that a buildup of carbon in the outlet of the reactor frequently resulted in a complete blocking during longer measurements due to the exothermic Boudouard equilibrium (eq. 2). Carbon formation is accelerating during the experiment. Formation of H_2O through the rWGS reaction is low at atmospheric pressure and increases with pressure. Despite the depletion of H_2 and associated formation of CO by the rWGS, we find a higher ratio of H_2:CO in the product composition at 10 and 20 bar than at atmospheric pressure towards the end

of the reaction time. This observation again correlates with the depletion of CO and the formation of carbon via the Boudouard reaction equilibrium (eq. 2).

Table 2 summarizes the catalytic data obtained with $NiAl_2O_4/Al_2O_3$ and the conventional steam reforming catalyst after 5 h on stream. In case of the reference catalyst, only 42, 44 and 32% of CH_4 initial conversion are reached at 1, 10 and 20 bar. Deactivation occurred, too, resulting in final degrees of conversion of 37, 32 and 29%, respectively. However, there is less accumulation of solid carbonaceous species in the reactor. With respect to product gas analysis it is found that the most important follow-up reaction in this case is the rWGS leading to very low H_2:CO ratios, especially when operating at 20 bar. In addition, the relatively high yield of H_2O at only moderate methane conversion indicates a considerable waste of H_2.

The observed loss of activity for both samples may be explained by a partial coking of the catalytically active surface. Yet, the main fraction of carbon, especially in case of the spinel-based catalyst, is deposited well downstream of the catalyst bed, where the temperature is lower and exothermic reactions, such as the Boudouard reaction, are favored. A solution could be to quench the reaction behind the catalyst bed to prevent consecutive reactions of H_2 and CO. Such a measure would certainly contribute to overcome the limitations of DRM at industrially relevant conditions.

Fig. 4 shows the axial temperature profiles that were recorded during DRM with a thermocouple in the inner steel tube. In all cases, a correlation between catalytic activity and temperature in the catalyst bed is found. Due to the strongly endothermic DRM reaction, a cold spot is formed that becomes more pronounced when high degrees of methane conversion are reached. The highest recorded temperature in the inert case is 803 °C, which is already lower than the oven temperature of 820 °C and a nearly isothermal zone of 5 cm lengths is found around the middle of the catalyst bed. The coldest spot in the spinel-catalyst bed recorded at 1 bar amounts to only 771 °C, which is considerably lower than 779 °C found at 20 bar. A comparison between both curves also shows that the oven is affected by the heat uptake by dry reforming, as the temperature before and after the bed is higher in case of 1 bar. Here, the temperature controller of the oven compensates for the reaction cooling by means of a higher heating duty. Similar trends are found for DRM at different pressures for the conventional steam reforming catalyst, except that the cold spots are less pronounced due to lower degrees of conversion (Table 2). Especially the highly active spinel-based catalyst does not allow for measurements in the differential regime at low degrees of conversions, since utilization of less than 10 mg would be impractical and the WHSV is already as high as $2.94*10^6$ L h^{-1} kg^{-1}. Therefore, cold spots are observed towards the entrance of the bed indicating that the reaction proceeds the fastest at those positions, where the reactant concentrations are highest. These observations clearly demonstrate that recording of the axial temperature profile is mandatory for a reliable kinetic comparison of highly active DRM catalysts. Further studies are in progress with additional rapid quenching of the effluent to eliminate consecutive reactions in the outlet of the reactor.

Conclusions

Our experiments showed that the strategy of preparing a supported $NiAl_2O_4$ spinel and reducing the sample to yield dispersed Ni nanoparticles creates a highly active catalyst for the dry reforming of methane. Higher pressures lead to lower degrees of conversion in agreement with thermodynamic predictions. An increased formation of water and carbonaceous species is observed, which is, however, partly due to reactions in downstream cooling sections being unrelated to the actual bed. The formation of carbon deposits towards the reactor exit is plausible considering the exothermicity of the Boudouard equilibrium that benefits from moderate temperatures.

References

[1] Düdder H, Kähler K, Krause B, Mette K, Kühl S, Behrens M, Scherer V, Muhler M (2014) Catal. Sci. Technol. 4:3317-3328.

[2] Titus J, Roussière T, Wasserschaff G, Schunk S, Milanov A, Schwab E, Wagner G, Oeckler O, Gläser R (2016) Catalysis Today 270:68-75.

[3] Rostrup-Nielsen JR (2004) Catalysis Reviews 46 (3-4):247–270.

[4] Schulz LA, Kahle LCS, Herrera Delgado K, Schunk SA, Jentys A, Deutschmann O, Lercher JA (2015) Applied Catalysis A: General 504:599-607

[5] Verykios XE (2003) International Journal of Hydrogen Energy 28:1045-1063.

[6] Shamsi A, Johnson CD (2003) Catalysis Today 84:17-25

[7] Djinovic P, Crnivec IGO, Pintar A (2015) Catalysis Today 253:155-162

[8] Mette K, Kühl S, Tarasov A, Lunkenbein T, Willinger MG, Kröhnert J, Wrabetz S, Trunschke A, Düdder H, Kähler K, Friedel-Ortega K, Muhler M, Schlögl R, Behrens M (2016) ASC Catal. 6:7238-7248

[9] Oyama ST, Hacarlioglu P, Gu Y, Lee D (2012) International Journal of Hydrogen Energy 37:10444-10450

[10] Misture ST, McDevitt KM, Glass KC, Edwards DD, Howe JY, Rector KD, He H, Vogel SC (2015) Catal. Sci. Technol. 5:4565-4574

[11] Benrabaa R, Barama A, Boukhlouf H, Guerrero-Caballero J, Rubbens A, Bordes-Richard E, Löfberg A, Vannier RN (2017) International Journal of Hydrogen Energy 42:12989-12996

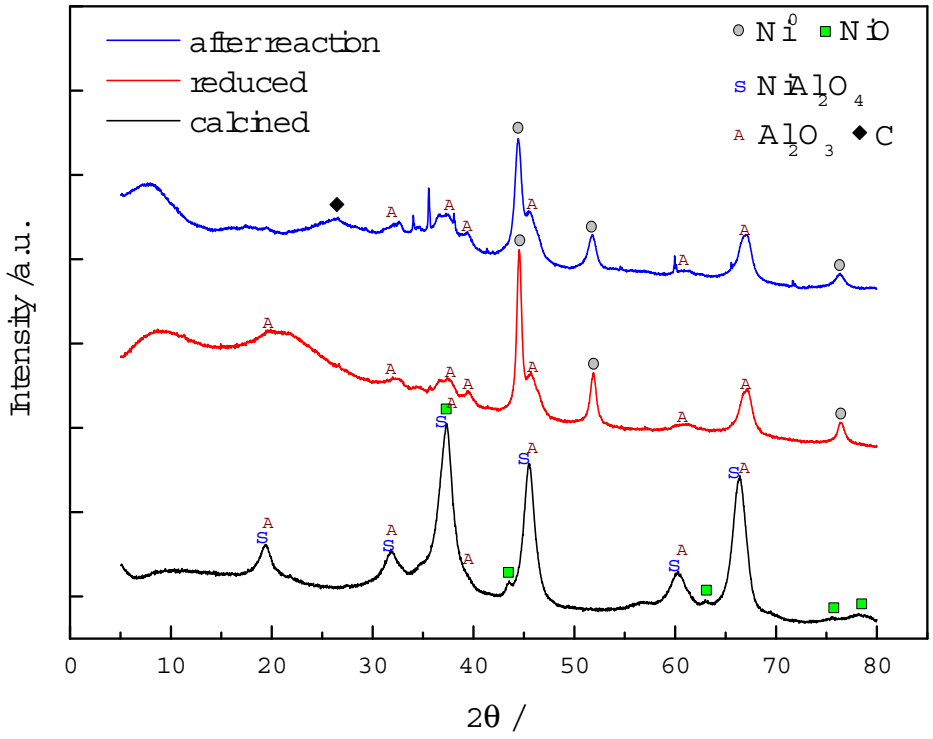

Figure 1. X-ray diffraction patterns of the $NiAl_2O_4/Al_2O_3$ catalyst calcined at 800 °C, reduced at 850 °C and after 15 h time on stream under DRM conditions at 820 °C and 1 bar.

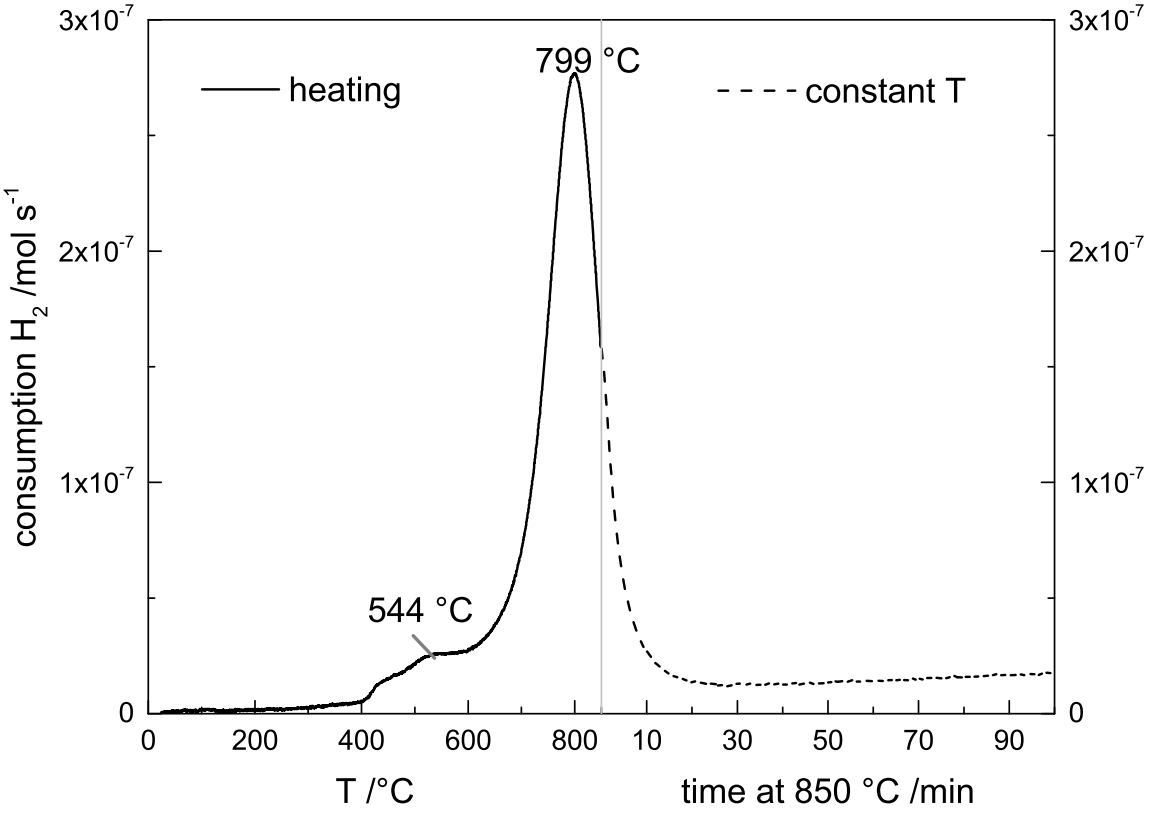

Figure 2. TPR profile of $NiAl_2O_4/Al_2O_3$ recorded at a constant heating rate of 6 K min^{-1} up to 850 °C and subsequent keeping of this temperature. Gas flow: 4.6 % H_2 in Ar, 84.1 mL min^{-1} total.

Table 1. Characterization results of $NiAl_2O_4/Al_2O_3$ obtained by ICP-OES, N_2 physisorption, H_2 chemisorption (bracketing plot), and XRD (Scherrer equation).

ICP-OES	N_2 physisorption	H_2 chemisorption		XRD
Ni [%]	a_{BET} [m^2g^{-1}]	Ni surface area [m^2g^{-1}]	Ni dispersion [%]	Ni Particle size [nm]
13.4	126	1.8	2.0	14.9

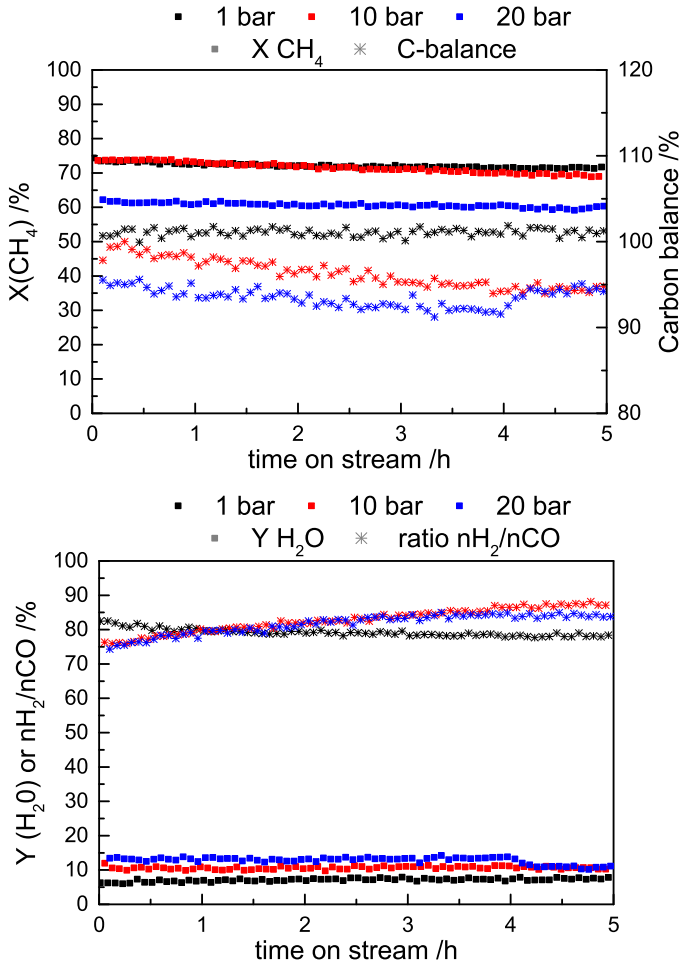

Figure 3. Catalytic test results using the reduced $NiAl_2O_4/Al_2O_3$ catalyst. Top: Degree of CH_4 conversion and carbon balance during 5 h of dry reforming at 820 °C. Bottom: Yield of water and H_2 / CO ratio.

Table 2. Catalytic test results obtained over both catalysts after 5 h at an oven temperature of 820 °C using a feed gas flow of 490 mL min^{-1}, CH_4:CO_2:N_2 = 7: 9.5:83.5.

	pressure [bar]	X CH_4 [%]	X CO_2 [%]	Y H_2 [%]	Y CO [%]	Y H_2O [%]	nH_2/nCO [%]	C balance [%]
$NiAl_2O_4/Al_2O_3$	1	72	66	62	70	8	78	100
$NiAl_2O_4/Al_2O_3$	10	69	57	58	57	10	87	94
$NiAl_2O_4/Al_2O_3$	20	60	47	46	47	11	84	94
Reforming catalyst	1	37	41	26	39	9	57	100
Reforming catalyst	10	31	35	23	33	8	60	99
Reforming catalyst	20	29	35	19	33	8	50	100

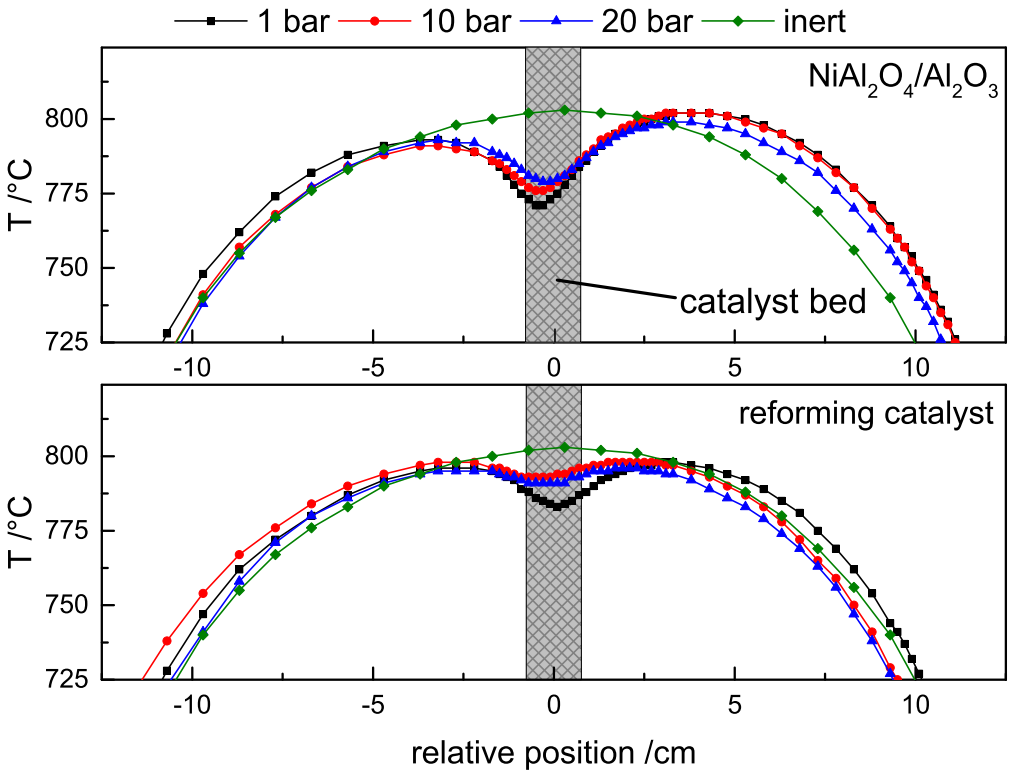

Figure 4. Axial temperature profiles, measured during DRM over $NiAl_2O_4/Al_2O_3$ and over the conventional steam reforming catalyst at an oven temperature of 820 °C at 1, 10 and 20 bar. The grey area represents the length of the catalyst bed. Position 0 cm is the middle of the bed. A profile recorded in exclusive nitrogen flow was added for comparison.